AN ASSESSMENT OF LEAST SQUARES FINITE ELEMENT MODELS WITH APPLICATIONS TO PROBLEMS IN HEAT TRANSFER AND SOLID MECHANICS

A Thesis

by

BRITTAN SHELDON PRATT

Submitted to the Office of Graduate Studies of
Texas A&M University
in partial fulfillment of the requirements for the degree of

MASTER OF SCIENCE

May 2008

Major Subject: Mechanical Engineering

AN ASSESSMENT OF LEAST SQUARES FINITE ELEMENT MODELS WITH APPLICATIONS TO PROBLEMS IN HEAT TRANSFER AND SOLID MECHANICS

A Thesis

by

BRITTAN SHELDON PRATT

Submitted to the Office of Graduate Studies of
Texas A&M University
in partial fulfillment of the requirements for the degree of

MASTER OF SCIENCE

Approved by:

Chair of Committee,	J. N. Reddy
Committee Members,	Anastasia Muliana
	Paul Roschke
Head of Department,	Dennis O'Neal

May 2008

Major Subject: Mechanical Engineering

ABSTRACT

An Assessment of Least Squares Finite Element Models with Applications to Problems in Heat Transfer and Solid Mechanics. (May 2008)

Brittan Sheldon Pratt, B.M.E., Grove City College

Chair of Advisory Committee: Dr. J.N. Reddy

Research is performed to assess the viability of applying the least squares model to one-dimensional heat transfer and Euler-Bernoulli Beam Theory problems. Least squares models were developed for both the full and mixed forms of the governing one-dimensional heat transfer equation along weak form Galerkin models. Both least squares and weak form Galerkin models were developed for the first order and second order versions of the Euler-Bernoulli beams.

Several numerical examples were presented for the heat transfer and Euler-Bernoulli beam theory. The examples for heat transfer included: a differential equation having the same form as the governing equation, heat transfer in a fin, heat transfer in a bar and axisymmetric heat transfer in a long cylinder. These problems were solved using both least squares models, and the full form weak form Galerkin model. With all four examples the weak form Galerkin model and the full form least squares model produced accurate results for the primary variables. To obtain accurate results with the mixed form least squares model it is necessary to use at least a quadratic polynominal. The least squares models with the appropriate approximation functions yielde more accurate results for the secondary variables than the weak form Galerkin..

The examples presented for the beam problem include: a cantilever beam with linearly varying distributed load along the beam and a point load at the end, a simply supported beam with a point load in the middle, and a beam fixed on both ends with

a distributed load varying cubically. The first two examples were solved using the least squares model based on the second order equation and a weak form Galerkin model based on the full form of the equation. The third problem was solved with the least squares model based on the second order equation. Both the least squares model and the Galerkin model calculated accurate results for the primary variables, while the least squares model was more accurate on the secondary variables.

In general, the least-squares finite element models yield more acurate results for gradients of the solution than the traditional weak form Galkerkin finite element models. Extension of the present assessment to multi-dimensional problems and nonlinear provelms is awaiting attention.

To My Parents

ACKNOWLEDGMENTS

I would like to thank my advisor Dr. J.N. Reddy for his insight, guidance and support. Without him, my thesis would not be what it is today.

I would also like to thank my colleagues, family and friends for their encouragement and support.

TABLE OF CONTENTS

CHAPTER Page

LIST OF TABLES

TABLE Page

LIST OF FIGURES

CHAPTER I

INTRODUCTION

A. Background

As scientists, mathematicians, and engineers have developed a better understanding of the world, there has been the push to simulate physical phenomena. Simulation of physical phenomena generally requires a mathematical model that describes it. Mathematical models of physical phenomena are derived using principles of physics, and they typically involve solving ordinary and/or partial differential equations. Analytical methods of solution of these equations exist for some simple geometries and/or boundaries conditions. Otherwise, solution of these equations requires the use of a numerical method, and the process is termed *numerical simulation.*

For over four decades, the finite element method has been widely applied to a variety of problems in solid mechanics, heat transfer, and fluid mechanics [1]. The traditional finite element analysis of a mathematical model is based on the weak form Galerkin method. Other methods including spectral, collocation, subdomain, and least squares have been developed [1, 2]. One of the major drawback of traditional finite element models based on weak form Galerkin method is the discontinuities introduce in the derivatives of the field variables at the inter-element boundaries. Such discontinuities are non-physical and introduce errors in the calculation of quantities based on the gradient of the solution (e.g., stresses and heat flux). A method that incorporates higher-order global differentiability of the solution in point-wise sense is desirable. This feature is essential to ensure that converged solutions indeed possess the same characteristics (in the point wise sense) as the theoretical solutions.

The journal model is *International Journal for Numerical Methods in Engineering.*

One such approach is the least squares method, which minimizes the error in the differential equation.

B. Least-Squares Formulation

The least squares method is based on the minimization of the integral of the square of the error introduced in the approximation of a differential equation. To illustrate the idea, we consider the linear operator equation [2]

$$A(u) - f = 0, \quad \text{in} \quad (0, L) \tag{1.1}$$

where A is a linear differential operator and f is a source term. Equation (1.1) is subjected to suitable boundary conditions on u and its derivative(s). Suppose that the dependent variable u is approximated by expression of the form

$$u \approx U = \sum_{j=1}^{n} \Delta_j \varphi_j(x) \tag{1.2}$$

where Δ_j are unknown parameters (related to the values of u and possibly its derivatives) and $\varphi_j(x)$ are suitably selected functions. Then

$$\mathcal{R} \equiv A(U) - f \neq 0, \quad \text{in} \quad (0, L) \tag{1.3}$$

where $\mathcal{R}$ is called the *residual*. The least squares method is a technique that determines Δ_j such that the integral of the square of the residual is a minimum. The integral of the square of the residual as given by

$$I(\Delta_j) = \int_0^L \mathcal{R}^2 \, dx \tag{1.4}$$

which is called the *least squares functional.* The necessary condition for a minimum of I is that its first derivative with respect to Δ_1, Δ_2, $\cdots$, Δ_n is zero:

$$0 = \delta I(\Delta_j) \equiv \frac{\partial I}{\partial \Delta_i} = 2 \int_0^L \mathcal{R} \, \frac{\partial \mathcal{R}}{\partial \Delta_i} \, dx, \quad \text{for} \quad i = 1, 2, \cdots, n \tag{1.5}$$

C. Present Study

The primary purpose of this thesis is to use set of one-dimensional problems from heat transfer and solid mechanics to evaluate least squares finite element models (LSFEM) and test their accuracy compared with the traditional weak form Galerkin finite element models.

Following this introduction, least-squares finite element models of heat transfer in one-dimensional systems and axial deformation of bars are presented in Chapter II. Both weak form Galerkin and least-squares finite element models are developed and numerical examples presented to illustrate the relative accuracy of various models. In Chapter III, weak form Galerkin and least-squares finite element models of the Euler–Bernoulli beam equations are outlined and several numerical examples are presented. Finally, in Chapter IV, summary and conclusions of the present work are outlined and some recommendations are included.

CHAPTER II

HEAT TRANSFER IN FINS AND AXIAL DEFORMATION OF BARS

Heat Transfer in fins, rods and long cylinders, and axial deformation of bars are governed by the same second order ordinary differential equation. Four models will be derived from the differential equation: the least squares model (LSFEMHT), the weak form Galerkin model (WGFEMHT), the mixed least squares model (MLSFEMHT) and the mixed weak form Galerkin model (MWGFEMHT). Four numerical examples with be solved using LSFEMHT, WGFEMHT, and MLSFEMHT and the accuracy of the different models will be compared.

A. Formulation

As model problems we use the following two sets of equations [1]:

$$-\frac{dv}{dx} + cu - f = 0, \quad v - a\frac{du}{dx} = 0 \tag{2.1}$$

The pair of equations (Eq.(2.1)) arise in a number of physical problems. Here we identify two problems. In heat transfer, the first equation represents the conservation of energy for one-dimensional systems (such as fins, plane walls, and axisymmetric geometries) and the second equation is the Fourier heat conduction law; u denotes temperature, v denotes the negative of heat, a is the product of conductivity and cross-sectional area of the fin ($a = kA$) in fins and plan, c is the product of heat transfer coefficient and perimeter of the fin ($c = \beta P$), and f is the internal heat generation. In solid mechanics, the first equation is the statement of conservation of linear momentum (or Newton's second law) and the second equation is the Hooke's law; u denotes axial displacement, a is the product of Young's modulus and area of

cross section ($a = EA$), v is the axial force, $c = 0$, and f is the axial distributed load.

$$-\frac{d}{dx}\left(a\frac{du}{dx}\right) + cu + f = 0 \tag{2.2}$$

The combination of the pair of equations given in Eq.(2.1) is referred to has the full equation (Eq. (2.2)). The pair of equations is referred to the mixed equations. A least squares formulation and weak form Galerkin formulation will be developed for full and mixed equations.

1. Least-Squares Model: LSFEMHT

Here we consider the full equation. In the finite element method, we divide the interval $(0, L)$ into a set of subintervals, called finite elements. A typical finite element is a line between x_a and x_b. The least-squares functional associated with Eq. (2.2) over a typical element is [we shall use u_h to represent the finite element approximation of u over (x_a, x_b)]

$$I_1(u_h) = \int_{x_a}^{x_b} [A(u_h) - f]^2 \, dx \tag{2.3}$$

The necessary condition for the minimum of I_1 is

$$0 = \delta I_1 = 2\int_{x_a}^{x_b} A(\delta u_h)\,[A(u_h) - f] \, dx \tag{2.4}$$

or

$$B(\delta u_h, u_h) = \ell(\delta u_h) \tag{2.5}$$

where $B(\cdot,\cdot)$ and $\ell(\cdot)$ denote the bilinear and linear forms

$$B(\delta u_h, u_h) = \int_{x_a}^{x_b} A(\delta u_h)\, A(u_h) \, dx, \quad \ell(\delta u_h) = \int_{x_a}^{x_b} A(\delta u_h)\, f \, dx \tag{2.6}$$

Since physics of problems described by Eq. (2.2) requires specification of u or $v = a(du/dx)$, it is necessary to seek an approximation of u such that the approx-

imation includes both u and its derivative du/dx as the nodal variables. Such an approximation over a typical element is provided by

$$u_h = \sum_{j=1}^{4} \Delta_j \, \varphi_j(x) \tag{2.7}$$

where Δ_1 and Δ_2 denotes the nodal values of u and $-(du/dx)$, respectively, at node 1, Δ_3 and Δ_4 denote the nodal values of u and $-(du/dx)$ at node 2, and φ_j denote the Hermite cubic polynomials [1]. Substitution of Eq. (2.7) into Eq. (2.6), we obtain the finite element model

$$[K^e]\{\Delta^e\} = \{F^e\}, \tag{2.8}$$

where

$$K^e_{ij} = B(\varphi_i, \varphi_j) = \int_{x_a}^{x_b} A(\varphi_i)\, A(\varphi_j)\; dx, \quad F^e_i = \ell(\varphi_i) = \int_{x_a}^{x_b} A(\varphi_i)\, f\; dx \tag{2.9}$$

2. Weak Form Galerkin Model: WKFEMHT

Here we consider finite element model based on the weak form of the full equation. The weak form is represented by

$$B(\delta u_h, u_h) = \ell(\delta u_h) \tag{2.10}$$

where $B(\cdot,\cdot)$ and $\ell(\cdot)$ denote the bilinear and linear forms

$$\begin{aligned} B(\delta u_h, u_h) &= \textstyle\int_{x_a}^{x_b} \left(a \frac{d\delta u_h}{dx} \frac{du_h}{dx} + c \delta u_h u_h \right) dx \\ \ell\left(\delta u_h\right) &= \textstyle\int_{x_a}^{x_b} \delta u_h \, f \; dx + \delta u_h(x_a) Q_1 + \delta u_h(x_b) Q_2, \end{aligned} \tag{2.11}$$

where

$$Q_1 = \left(-a \frac{du_h}{dx} \right)_{x_a}, \quad Q_2 = \left(a \frac{du_h}{dx} \right)_{x_b} \tag{2.12}$$

Since Q_i represent the nodal secondary variables (e.g., nodal heats or forces), it is only necessary to approximate the primary variable u_h with Lagrange approximation

$$u_h = \sum_{j=1}^{n} u_j \, \psi_j(x) \tag{2.13}$$

Substitution of Eq. (2.13) into Eq. (2.11), we obtain the finite element model

$$[K^e] \{u^e\} = \{F^e\}, \tag{2.14}$$

where

$$\begin{aligned} K^e_{ij} &= B(\psi_i, \psi_j) = \textstyle\int_{x_a}^{x_b} \left(a \frac{d\psi_i}{dx} \frac{d\psi_j}{dx} + c \psi_i \psi_j \right) dx \\ F^e_i &= \ell(\psi_i) = \textstyle\int_{x_a}^{x_b} \psi_i \, f \; dx + \psi_i(x_a) Q_1 + \psi_i(x_b) Q_2 \end{aligned} \tag{2.15}$$

3. Mixed Least-Squares Model: MLSFEMHT

Next, we consider the mixed equations in Eq. (2.1). The least-squares functional associated with Eq. (2.1) over a typical element is

$$I_2(u_h, v_h) = \int_{x_a}^{x_b} \left[\left(-\frac{dv_h}{dx} + c u_h - f \right)^2 + \left(v_h - a \frac{du_h}{dx} \right)^2 \right] \, dx \tag{2.16}$$

The necessary condition for the minimum of I_2 is

$$0 = \int_{x_a}^{x_b} \left[\left(-\frac{d\delta v_h}{dx} + c \delta u_h \right) \left(-\frac{dv_h}{dx} + cu - f \right) + \left(\delta v_h - a \frac{d\delta u_h}{dx} \right) \left(v_h - a \frac{du_h}{dx} \right) \right] \, dx \tag{2.17}$$

The above statement is equivalent to the following equations (since δu_h and δv_h are independent of each other, collect the expressions involving δu_h and δv_h separately and set them to zero):

$$\begin{aligned} 0 &= \textstyle\int_{x_a}^{x_b} \left[c \delta u_h \left(-\frac{dv_h}{dx} + c u_h - f \right) - a \frac{d\delta u_h}{dx} \left(v_h - a \frac{du_h}{dx} \right) \right] \, dx \\ 0 &= \textstyle\int_{x_a}^{x_b} \left[-\frac{d\delta v_h}{dx} \left(-\frac{dv_h}{dx} + cu - f \right) + \delta v_h \left(v_h - a \frac{du_h}{dx} \right) \right] \, dx \end{aligned} \tag{2.18}$$

Since both u and $v = a(du/dx)$, are included in the formulation, it is sufficient to seek approximations of the form

$$u_h = \sum_{j=1}^{m} u_j \, \psi_j^{(1)}(x), \quad v_h = \sum_{j=1}^{n} v_j \, \psi_j^{(2)}(x) \tag{2.19}$$

where u_j and v_j denote the nodal values of u and v, respectively, at jth node, and $\psi_j^{(1)}$ and $\psi_j^{(2)}$ are the Lagrange interpolation functions of degree $(m-1)$ and $(n-1)$, respectively. Substitution of Eq. (2.19) into Eq. (2.18), we obtain the finite element model

$$\begin{bmatrix} [K^{11}] & [K^{12}] \\ [K^{12}]^\top & [K^{22}] \end{bmatrix} \begin{Bmatrix} \{u\} \\ \{v\} \end{Bmatrix} = \begin{Bmatrix} \{F^1\} \\ \{F^2\} \end{Bmatrix} \tag{2.20}$$

where

$$\begin{aligned} K_{ij}^{11} &= \int_{x_a}^{x_b} \left(c^2 \psi_i^{(1)} \psi_j^{(1)} + a^2 \tfrac{d\psi_i^{(1)}}{dx} \tfrac{d\psi_j^{(1)}}{dx} \right) dx \\ K_{ij}^{12} &= -\int_{x_a}^{x_b} \left(c \psi_i^{(1)} \tfrac{d\psi_j^{(2)}}{dx} + a \tfrac{d\psi_i^{(1)}}{dx} \psi_j^{(2)} \right) dx \\ K_{ij}^{21} &= -\int_{x_a}^{x_b} \left(c \tfrac{d\psi_i^{(2)}}{dx} \psi_j^{(1)} + a \psi_i^{(2)} \tfrac{d\psi_j^{(1)}}{dx} \right) dx \\ K_{ij}^{22} &= \int_{x_a}^{x_b} \left(\psi_i^{(2)} \psi_j^{(2)} + \tfrac{d\psi_i^{(2)}}{dx} \tfrac{d\psi_j^{(2)}}{dx} \right) dx \\ F_i^1 &= \int_{x_a}^{x_b} c f \, \psi_i^{(1)} \, dx, \quad F_i^2 = -\int_{x_a}^{x_b} f \, \tfrac{d\psi_i^{(2)}}{dx} \, dx \end{aligned} \tag{2.21}$$

4. Mixed Weak Form Galerkin Model: MWKFEMHT

Consider the mixed equations in Eq. (2.1). The weak forms of the pair over a typical element are

$$\begin{aligned} 0 &= \int_{x_a}^{x_b} \left(\tfrac{d\delta u_h}{dx} v_h + c \delta u_h u_h - f \right) \, dx - \delta u_h(x_a)[-v(x_a)] - \delta u_h(x_b) v(x_b) \\ 0 &= \int_{x_a}^{x_b} \left(\delta v_h \tfrac{du_h}{dx} - \tfrac{1}{a} \delta v_h \, v_h \right) \, dx \end{aligned} \tag{2.22}$$

We seek approximations of the form

$$u_h = \sum_{j=1}^{m} u_j \, \psi_j^{(1)}(x), \quad v_h = \sum_{j=1}^{n} v_j \, \psi_j^{(2)}(x) \tag{2.23}$$

where u_j and v_j denote the nodal values of u and v, respectively, at jth node, and $\psi_j^{(1)}$ and $\psi_j^{(2)}$ are the Lagrange interpolation functions of degree $(m-1)$ and $(n-1)$, respectively. Substitution of Eq. (2.23) into Eq. (2.22), we obtain the finite element model

$$\begin{bmatrix} [K^{11}] & [K^{12}] \\ [K^{12}]^\top & [K^{22}] \end{bmatrix} \begin{Bmatrix} \{u\} \\ \{v\} \end{Bmatrix} = \begin{Bmatrix} \{F^1\} \\ \{F^2\} \end{Bmatrix} \tag{2.24}$$

where

$$\begin{aligned} K_{ij}^{11} &= \textstyle\int_{x_a}^{x_b} c\,\psi_i^{(1)}\psi_j^{(1)}\,dx, & K_{ij}^{12} &= \textstyle\int_{x_a}^{x_b} \frac{d\psi_i^{(1)}}{dx}\psi_j^{(2)}\,dx \\ K_{ij}^{21} &= \textstyle\int_{x_a}^{x_b} \psi_i^{(2)}\frac{d\psi_j^{(1)}}{dx}\,dx, & K_{ij}^{22} &= -\textstyle\int_{x_a}^{x_b} \frac{1}{a}\psi_i^{(2)}\psi_j^{(2)}\,dx \\ F_i^1 &= \textstyle\int_{x_a}^{x_b} f\,\psi_i^{(1)}\,dx + \psi_i^{(1)}(x_a)V_1 + \psi_i^{(1)}(x_b)V_2, & F_i^2 &= 0 \end{aligned} \tag{2.25}$$

5. Axisymmetric Geometries

The mixed and full equations, Eqs. (2.1) and (2.2) respectively apply to axisymmetric geometries also. The only differences is a is now the product of conductivity and radial location and the dx terms are transformed into dr. The formulations given in Eqs (2.9), (2.15), (2.21) and (2.25) are still valid assuming one changes the dx terms to dr.

B. Numerical Examples

1. Problem 1: Solution of a Differential Equation

Given the differential equation:

$$-\frac{d^2u}{dx^2} - u + x^2 = 0 \tag{2.26}$$

Over the domain $0 < x < 1$, solve it for the given boundary conditions:

$$u\,(0) = 0, \quad u\,(1) = 0 \tag{2.27}$$

The problem has been solving using the WGFEM formulation four linear elements, two and quadratic elements. It was also solved using a four hermite element LSFEMHT and four linear and quadratic element MLSFEMHT. The results of the primary varable can be found in Table I.

Table I. Results for the Negative Primary Variable (-10$u(x)$)

		WGFEM†			LSFEMHT	MLSFEMHT		
x	Exact†	4L	2Q	4Q	4H	4L	8L	4Q
0.0000	0.0000	0.0000	0.0000	0.0000	0.0000	0.0000	0.0000	0.0000
0.1250	0.1192			0.1193			0.1217	0.1196
0.2500	0.2337	0.2323	0.2345	0.2337	0.2338	0.2495	0.2378	0.2338
0.3750	0.3345			0.3345			0.3393	0.3345
0.5000	0.4076	0.4052	0.4078	0.4076	0.4076	0.4263	0.4124	0.4077
0.6250	0.4350			0.4353			0.4391	0.4353
0.7500	0.3942	0.3919	0.3947	0.3942	0.3942	0.4057	0.3971	0.3942
0.8750	0.2590			0.2591			0.2606	0.2593
1.0000	0.0000	0.0000	0.0000	0.0000	0.0000	0.0000	0.0000	0.0000

†Results taken from Reddy's *An Introduction to the Finite Element Method.* [1]

2. Problem 2: Heat Transfer in a Fin

Consider heat transfer in a fin (see Fig. 1. The fin is 100 mm long, 1 mm high and 5 mm wide. The thermal conductivity of the fin is 385 $\frac{W}{m\cdot^\circ C}$. There is a specified temperature at the base of the fin of 100$^\circ C$. There is convection along the length of the fin with convection coefficient of 25 $\frac{W}{m^2\cdot^\circ C}$ and the ambient temperature is 20$^\circ C$.

The are two different boundary conditions for the end of the fin, the first is convection and the second is a specified temperature of $20°C$.

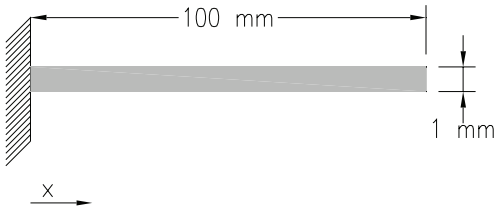

Fig. 1. Heat Transfer in a Fin.

The problem with the first set of boundary conditions has been solved using the WGFEMHT with four and eight linear elements and two and four quadratic elements. The temperature results are given in Table II. It has been solved using LSFEMHT with two and four hermite elements. It has been solved using MLSFEMHT with four and eight linear elements and two and four quadratic elements. The temperature results are in Table III. The results of the heat flux at the interface of the body and the fin are given in Table IV.

Table II. Temperature ($°C$) Results for Boundary Condition Set 1 Using WGFEM

x	Exact†	WGFEM			
		4L†	2Q	8L	4Q
0.0000	100.000	100.000	100.000	100.000	100.000
0.0125	90.331			90.317	90.332
0.0250	82.377	82.283	82.374	82.354	82.316
0.0375	75.946			75.915	76.003
0.0500	70.880	70.732	70.884	70.843	70.846
0.0625	67.055			67.015	67.156
0.0750	64.379	64.204	64.380	64.335	64.407
0.0875	62.785			62.740	62.939
0.1000	62.236	62.053	62.240	62.190	62.329

†Results taken from Reddy's *An Introduction to the Finite Element Method.* [1]

The temperature of the problem with the second set of boundary conditions has been calculated using WFEMHT with four linear elements, LSFEMHT with four hermite elements and MLSFEMHT with four linear and quadratic elements. The results are given in Table V. The heat flux has been calculated and can be found in Figure 2.

Table III. Temperature ($°C$) Results for Boundary Condition Set 1 Using LSFEMHT and MLSFEM

x	Exact†	LSFEMHT		MLSFEMHT			
		2H	4H	4L	2Q	8L	4Q
0.0000	100.000	100.000	100.00	100.000	100.000	100.000	100.000
0.0125	90.331					91.560	90.485
0.0250	82.377		82.415	88.483	82.619	84.483	82.346
0.0375	75.946					78.665	76.402
0.0500	70.880	70.964	70.958	80.337	70.386	74.018	70.832
0.0625	67.055					70.469	67.118
0.0750	64.379		64.505	75.471	64.909	67.964	64.323
0.0875	62.785					66.463	62.833
0.1000	62.236	62.429	62.422	73.822	61.644	65.944	62.178

†Results taken from Reddy's *An Introduction to the Finite Element Method.* [1]

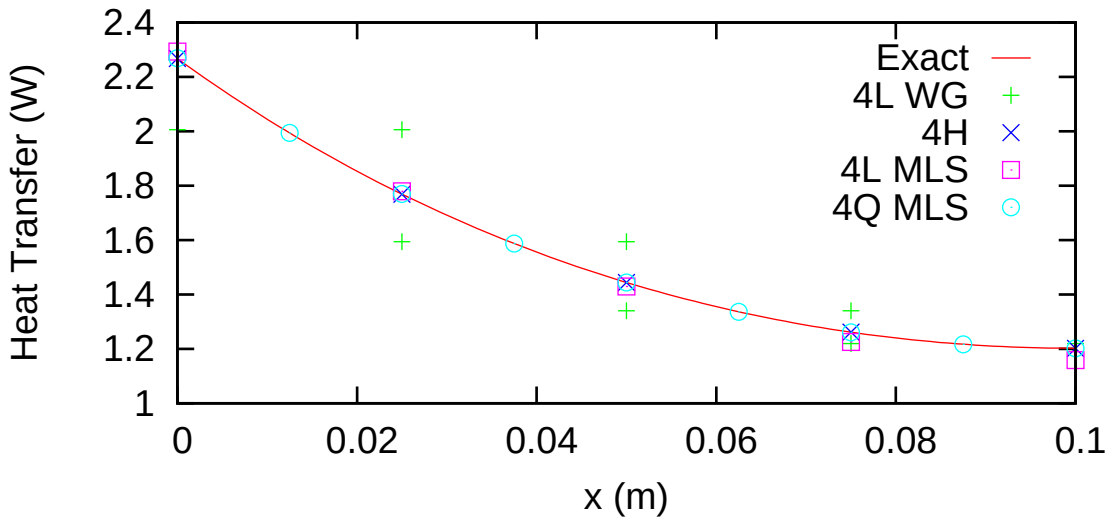

Fig. 2. The Heat Transfer for the Second Set of Boundary Conditions.

Table IV. Heat Transfer (-W) Results at x=0mm for Boundary Condition Set 1

	Heat Transfer (-W)
Exact Solution†	1.6300
4L WGFEMHT†	1.6420
2Q WGFEMHT	1.6420
2H LSFEMHT	1.6295
4H LSFEMHT	1.6299
4L MLSFEMHT	1.8880
2Q MLSFEMHT	1.6464
8L MLSFEMHT	1.7171
4Q MLSFEMHT	1.6341

†Results taken from Reddy's *An Introduction to the Finite Element Method.* [1]

Table V. Temperature ($^{\circ}C$) Results for Boundary Condition Set 2

		WGFEMHT	LSFEMHT	MLSFEMHT	
x	Exact†	4L†	4H	4L	4Q
0.0000	100.000	100.000	100.00	100.000	100.000
0.0250	74.000	73.955	73.999	76.952	73.982
0.0500	53.333	53.252	53.300	56.514	53.282
0.0750	35.870	35.842	35.870	37.821	35.860
0.1000	20.000	20.000	20.000	20.000	20.000

†Results taken from Reddy's *An Introduction to the Finite Element Method.* [1]

3. Problem 3: Heat Transfer in a Bar

Consider heat transfer in a bar (see Fig. 3). The bar is 0.5m long with a diameter of 0.02m. The thermal conductivity of the bar is 50 $\frac{W}{m\cdot^\circ C}$. On the left end of the bar there is a specified temperature of 300°C. Along the circumference of the bar there is convection. The convection heat transfer coefficient is 100 $\frac{W}{m^2\cdot^\circ C}$ and the ambient temperature is 20°C. The right end of the bar is insulated.

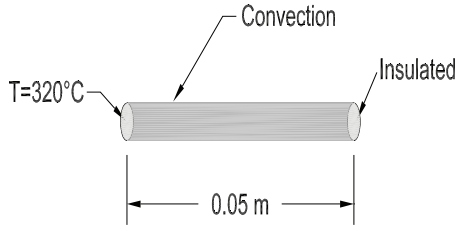

Fig. 3. Heat Transfer in a Rod.

The temperature has been calculated using the finite difference method (FDM) with two and four linear elements, WGFEMHT with two and four linear elements, LSFEMHT with two hermite elements and MLSFEMHT with four linear and two quadratic elements. The results are given in Table VI.

4. Problem 4: Axisymmetric Heat Transfer in a Long Cylinder

Consider a long solid cylinder with a outer diameter of 0.01m (see Fig 4). The thermal conductivity of the cylinder is 20 $\frac{W}{m\cdot^\circ C}$. There is a constant internal heat generation rate of 2x10^8 $\frac{W}{m^3}$. The outer diameter has a specified temperature of 100°C.
The problem has been solved using the WGFEMHT with four and eight linear elements, LSFEMHT with four and eight hermite elements and with MLSFEMHT using eight linear and four quadratic elements. The temperature results are given in Table VII. Table VIII shows the calculated heat transfer at the outer radius.

Table VI. Temperature ($°C$) Results for Problem 3

x	Exact†	FDM†		WGFEMHT†		LSFEMHT	MLSFEMHT	
		2L	4L	2L	4L	2H	4L	2Q
0.0000	300.00	300.00	300.00	300.00	300.00	300.00	300.00	300.00
0.1250	251.71		251.52		251.89		277.33	255.90
0.2500	219.23	217.98	218.92	220.41	219.53	219.24	261.00	217.89
0.3750	200.52		200.16		200.89		251.14	202.91
0.5000	194.42	192.83	194.03	195.92	194.80	194.43	247.85	192.74

†Results taken from Reddy's *An Introduction to the Finite Element Method*. [1]

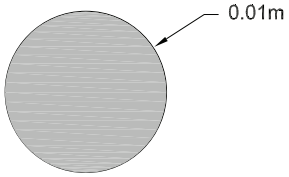

Fig. 4. Axisymmetric Heat Transfer in a Long Cylinder.

Table VII. Temperature ($^{\circ}C$) Results for Problem 4

		WGFEM		LSFEMHT		MLSFEMHT	
$\frac{r}{R_0}$	Exact†	4L†	8L†	4H	8H	8L	4Q
0.000	350.00	358.73	352.63	350.00	350.00	359.14	350.00
0.125	346.09		347.42		346.09	351.33	346.09
0.250	334.38	337.90	335.25	334.38	334.38	337.94	334.37
0.375	314.84		315.48		314.84	317.38	314.84
0.500	287.50	289.29	287.50	287.50	287.50	289.30	287.50
0.625	252.34		252.65		252.34	253.56	252.34
0.750	209.38	210.45	209.56	209.38	209.38	210.12	209.37
0.875	158.59		158.68		158.59	158.94	158.59
1.000	100.00	100.00	100.00	100.00	100.00	100.00	100.00

†Results taken from Reddy's *An Introduction to the Finite Element Method.* [1]

Table VIII. Heat Transfer (W) Results at r=R^o

	Heat Transfer (-W)
Exact Solution†	62.832
4L WGFEMHT	58.992
8L WGFEMHT	55.351
4H LSFEMHT	62.832
8H LSFEMHT	62.832
8L MLSFEMHT	62.832
4Q MLSFEMHT	62.832

†Results taken from Reddy's *An Introduction to the Finite Element Method.* [1]

C. Conclusions

The LSFEMHT, WGFEMHT models accurately calculate the primary variables regardless of the order of the approximating shape function . For the MLSFEMHT model to calculate accurate results with a reasonible number of elements, it is recommended to use at least a second order approximating shape function. The LSFEMHT and MLSFEMHT models have two degrees of freedom per node while the WGFEMHT has one. When the the three models are compared based on the number of degrees of freedom the are all comparable. THe LSFEMHT and MLSFEMHT models accurately compute the secondary variables while the WGFEMHT does not. The MWGFEMHT has been included for completeness of the formulation. Future work will include implimention of the MWGFEMHT model and producing numerical results.

CHAPTER III

EULER-BERNOULLI BEAM THEORY

The Euler-Bernoulli Beam Theory is descripted by a fourth order ordinary differential equation. Four models will be derived from the differential equation: the second order mixed least squares model from (MLSFEMEB1), the second order weak form Galerkin model (MWGFEMEB1), the first order mixed least squares model from (MLSFEMEB2) and the first order weak form Galerkin model (MWGFEMEB2). Three numerical examples with be solved using MLSFEMEB1 and a weak form Galerkin model (WGFEMEB) which can be in Reddy's book titled An Introduction to the Finite Element Method. [1] and the accuracy of the two models will be compared.

A. Formulation

The Euler-Bernoulli Beam Theory is given in Eq. (3.1).

$$-\frac{d^2M}{dx^2} + kw - q = 0, \quad \frac{M}{b} + \frac{d^2w}{dx^2} = 0 \tag{3.1}$$

The pair of equations (Eq. (3.1)) arise in bending of beams according to the euler-bernoulli beam theory, where the first equation represents equilibrium of transverse forces on the beam, and the second equation is a constitutive equation (moment-deflection relation); here w denotes the transverse deflection, m the bending moment, q the transversely distributed load, k the modulus of elastic foundation, and b is the product of young's modulus and second moment of area ($b = ei$).

1. Least-squares Model: MLSFEMEB1

The least-squares functional associated with Eq. (3.1) over a typical element is

$$J_1(w_h, M_h) = \int_{x_a}^{x_b} \left[\left(-\frac{d^2 M_h}{dx^2} + k w_h - q \right)^2 + \left(\frac{M_h}{b} + \frac{d^2 w_h}{dx^2} \right)^2 \right] \, dx \tag{3.2}$$

The necessary condition for the minimum of J_1 is

$$0 = \int_{x_a}^{x_b} \left[\left(-\frac{d^2 \delta M_h}{dx^2} + k \delta w_h \right) \left(-\frac{d^2 M_h}{dx^2} + k w_h - q \right) + \left(\frac{\delta M_h}{b} + \frac{d^2 \delta w_h}{dx^2} \right) \left(\frac{M_h}{b} + \frac{d^2 w_h}{dx^2} \right) \right] \, dx \tag{3.3}$$

As before, the above statement is equivalent to the following equations:

$$\begin{aligned} 0 &= \textstyle\int_{x_a}^{x_b} \left[k \delta w_h \left(-\frac{d^2 M_h}{dx^2} + k w_h - q \right) + \frac{d^2 \delta w_h}{dx^2} \left(\frac{M_h}{b} + \frac{d^2 w_h}{dx^2} \right) \right] \, dx \\ 0 &= \textstyle\int_{x_a}^{x_b} \left[-\frac{d^2 \delta M_h}{dx^2} \left(-\frac{d^2 M_h}{dx^2} + k w_h - q \right) + \frac{\delta M_h}{b} \left(\frac{M_h}{b} + \frac{d^2 w_h}{dx^2} \right) \right] \, dx \end{aligned} \tag{3.4}$$

Since the physics of the Euler-Bernoulli beam theory requires the specification of w, $\theta = -(dw/dx)$, M, and $V = (dM/dx)$, we seek Hermite cubic approximation of both w_h and M_h

$$w_h = \sum_{j=1}^{4} \Delta_j^1 \, \varphi_j(x), \quad M_h = \sum_{j=1}^{4} \Delta_j^2 \, \varphi_j(x) \tag{3.5}$$

where Δ_j^1 and Δ_j^2 denote the nodal values of $(w_h, \, -dw_h/dx)$ and $(M_h, -dM/dx)$ respectively, at the jth node, and φ_j are the Hermite cubic interpolation functions. Substitution of Eq. (3.5) into Eq. (3.4), we obtain the finite element model

$$\begin{bmatrix} [K^{11}] & [K^{12}] \\ [K^{12}]^\top & [K^{22}] \end{bmatrix} \begin{Bmatrix} \{\Delta^1\} \\ \{\Delta^2\} \end{Bmatrix} = \begin{Bmatrix} \{F^1\} \\ \{F^2\} \end{Bmatrix} \tag{3.6}$$

where

$$\begin{aligned} K_{ij}^{11} &= \int_{x_a}^{x_b} \left(k^2 \varphi_i \varphi_j + \tfrac{d^2\varphi_i}{dx^2} \tfrac{d^2\varphi_j}{dx^2} \right) dx \\ K_{ij}^{12} &= \int_{x_a}^{x_b} \left(\tfrac{1}{b} \tfrac{d^2\varphi_i}{dx^2} \varphi_j - k \varphi_i \tfrac{d^2\varphi_j}{dx^2} \right) dx \\ K_{ij}^{21} &= \int_{x_a}^{x_b} \left(\tfrac{1}{b} \varphi_i \tfrac{d^2\varphi_j}{dx^2} - k \tfrac{d^2\varphi_i}{dx^2} \varphi_j \right) dx \\ K_{ij}^{22} &= \int_{x_a}^{x_b} \left(\tfrac{1}{b^2} \varphi_i \varphi_j + \tfrac{d^2\varphi_i}{dx^2} \tfrac{d^2\varphi_j}{dx^2} \right] dx \\ F_i^1 = \int_{x_a}^{x_b} kq\, \varphi_i \, dx, &\quad F_i^2 = \int_{x_a}^{x_b} q\, \tfrac{d^2\varphi_i}{dx^2} \, dx \end{aligned} \tag{3.7}$$

2. Weak Form Galerkin Model: MWKFEMEB1

We consider the pair of equations involving w and M Eq. 3.1)). The weak forms of the equations over a typical element are

$$\begin{aligned} 0 &= \int_{x_a}^{x_b} \left(k \delta w_h w_h + \tfrac{d\delta w_h}{dx} \tfrac{dM_h}{dx} - \delta w_h \, q \right) \, dx - \delta w_h(x_a) \left[-\tfrac{dM_h}{dx} \right]_{x_a} - \delta w_h(x_b) \left[\tfrac{dM_h}{dx} \right]_{x_b} \\ 0 &= \int_{x_a}^{x_b} \left(\tfrac{d\delta M_h}{dx} \tfrac{dw_h}{dx} - \tfrac{1}{b} \delta M_h \, M_h \right) \, dx - \delta M_h(x_a) \left[-\tfrac{dw_h}{dx} \right]_{x_a} - \delta M_h(x_b) \left[\tfrac{dw_h}{dx} \right]_{x_b} \end{aligned} \tag{3.8}$$

We note that (w, M) are the primary variables and ($V_h = dM_h/dx$, $\theta = -(dw/dx)$) are the secondary variables of this mixed weak form model. The model admits Lagrange approximation of both w_h and M_h

$$w_h = \sum_{j=1}^{4} w_j \, \psi_j^{(1)}(x), \quad M_h = \sum_{j=1}^{4} M_j \, \psi_j^{(2)}(x) \tag{3.9}$$

where w_j and M_j denote the nodal values of w_h and M_h respectively, at the jth node. Substitution of Eq. (3.9) into Eq. (3.8), we obtain the finite element model

$$\begin{bmatrix} [K^{11}] & [K^{12}] \\ [K^{12}]^\top & [K^{22}] \end{bmatrix} \begin{Bmatrix} \{w\} \\ \{M\} \end{Bmatrix} = \begin{Bmatrix} \{F^1\} \\ \{F^2\} \end{Bmatrix} \tag{3.10}$$

where

$$\begin{gathered} K_{ij}^{11} = \int_{x_a}^{x_b} k\,\psi_i^{(1)}\psi_j^{(1)}\,dx, \quad K_{ij}^{12} = \int_{x_a}^{x_b} \frac{d\psi_i^{(1)}}{dx}\frac{d\psi_j^{(2)}}{dx}\,dx \\ K_{ij}^{21} = \int_{x_a}^{x_b} \frac{d\psi_i^{(2)}}{dx}\frac{d\psi_j^{(1)}}{dx}\,dx, \quad K_{ij}^{22} = -\int_{x_a}^{x_b} \tfrac{1}{b}\psi_i^{(2)}\psi_j^{(2)}\,dx \\ F_i^1 = \int_{x_a}^{x_b} q\,\psi_i^{(1)}\,dx + \psi_i^{(1)}(x_a)V_1 + \psi_i^{(1)}(x_b)V_2 \\ F_i^2 = \psi_i^{(2)}(x_a)\Theta_1 + \psi_i^{(2)}(x_b)\Theta_2 \end{gathered} \tag{3.11}$$

3. Least-squares Model: MLSFEMEB2

Here rewrite the set of equations in Eq. (3.1) as a set of four first-order equations

$$-\frac{dV}{dx} + kw - q = 0, \quad \theta + \frac{dw}{dx} = 0, \quad \frac{M}{b} - \frac{d\theta}{dx} = 0, \quad -V + \frac{dM}{dx} = 0 \tag{3.12}$$

The least-squares functional associated with the above four equations over a typical element is

$$\begin{aligned} J_2(w_h, \theta_h, M_h, V_h) = \int_{x_a}^{x_b} \Big[&\Big(-\tfrac{dV_h}{dx} + kw_h - q\Big)^2 + \Big(\theta_h + \tfrac{dw_h}{dx}\Big)^2 \\ &+ \Big(\tfrac{M_h}{b} - \tfrac{d\theta_h}{dx}\Big)^2 + \Big(-V_h + \tfrac{dM_h}{dx}\Big)^2 \Big]\,dx \end{aligned} \tag{3.13}$$

The necessary condition for the minimum of J_2 is

$$\begin{aligned} 0 = \int_{x_a}^{x_b} \Big[&\Big(-\tfrac{d\delta V_h}{dx} + k\delta w_h\Big)\Big(-\tfrac{dV_h}{dx^2} + kw_h - q\Big) + \Big(\delta\theta_h + \tfrac{d\delta w_h}{dx}\Big)\Big(\theta_h + \tfrac{dw_h}{dx}\Big) \\ &+ \Big(\tfrac{\delta M_h}{b} - \tfrac{d\delta\theta_h}{dx}\Big)\Big(\tfrac{M_h}{b} - \tfrac{d\theta_h}{dx}\Big) + \Big(-\delta V_h + \tfrac{d\delta M_h}{dx}\Big)\Big(-V_h + \tfrac{dM_h}{dx}\Big)\Big]\,dx \end{aligned} \tag{3.14}$$

The four statements associated with the statement in Eq. (3.14) are:

$$\begin{gathered} 0 = \int_{x_a}^{x_b} \Big[k\delta w_h\Big(-\tfrac{dV_h}{dx} + kw_h - q\Big) + \tfrac{d\delta w_h}{dx}\Big(\theta_h + \tfrac{dw_h}{dx}\Big)\Big]\,dx \\ 0 = \int_{x_a}^{x_b} \Big[\delta\theta_h\Big(\theta_h + \tfrac{dw_h}{dx}\Big) - \tfrac{d\delta\theta_h}{dx}\Big(\tfrac{M_h}{b} - \tfrac{d\theta_h}{dx}\Big)\Big]\,dx \\ 0 = \int_{x_a}^{x_b} \Big[\tfrac{\delta M_h}{b}\Big(\tfrac{M_h}{b} - \tfrac{d\theta_h}{dx}\Big) + \tfrac{d\delta M_h}{dx}\Big(-V_h + \tfrac{dM_h}{dx}\Big)\Big]\,dx \\ 0 = \int_{x_a}^{x_b} \Big[-\tfrac{d\delta V_h}{dx}\Big(-\tfrac{dV_h}{dx} + kw_h - q\Big) - \delta V_h\Big(-V_h + \tfrac{dM_h}{dx}\Big)\Big]\,dx \end{gathered} \tag{3.15}$$

In this model, all physical variables that enter the specification of the boundary conditions appear as unknowns. Hence, they all can be approximated by Lagrange

interpolation functions. Let

$$\begin{aligned} w_h &= \textstyle\sum_{j=1}^{m} w_j\, \psi_j^{(1)}(x), \quad \theta_h = \sum_{j=1}^{n} \theta_j\, \psi_j^{(2)}(x), \\ M_h &= \textstyle\sum_{j=1}^{p} M_j\, \psi_j^{(3)}(x), \quad V_h = \sum_{j=1}^{q} V_j\, \psi_j^{(4)}(x), \end{aligned} \tag{3.16}$$

where w_j, θ_j, M_j, and V_j denote the nodal values of w_h, θ_h, M_h, and V_h, respectively, at the jth node. Substitution of Eq. (3.16) into Eq. (3.15), we obtain the finite element model

$$\begin{bmatrix} [K^{11}] & [K^{12}] & [K^{13}] & [K^{14}] \\ [K^{12}]^\top & [K^{22}] & [K^{23}] & [K^{24}] \\ [K^{13}]^\top & [K^{23}]^\top & [K^{33}] & [K^{34}] \\ [K^{14}]^\top & [K^{24}]^\top & [K^{34}]^\top & [K^{44}] \end{bmatrix} \begin{Bmatrix} \{u\} \\ \{\theta\} \\ \{M\} \\ \{V\} \end{Bmatrix} = \begin{Bmatrix} \{F^1\} \\ \{F^2\} \\ \{F^3\} \\ \{F^4\} \end{Bmatrix} \tag{3.17}$$

where

$$\begin{gathered} K_{ij}^{11} = \int_{x_a}^{x_b} \left(k^2 \psi_i^{(1)} \psi_j^{(1)} + \tfrac{d\psi_i^{(1)}}{dx} \tfrac{d\psi_j^{(1)}}{dx} \right) dx, \quad K_{ij}^{12} = \int_{x_a}^{x_b} \tfrac{d\psi_i^{(1)}}{dx} \psi_j^{(2)}\, dx, \\ K_{ij}^{13} = 0, \quad K_{ij}^{14} = -\int_{x_a}^{x_b} k\, \psi_i^{(1)} \tfrac{d\psi_j^{(4)}}{dx}\, dx, \quad K_{ij}^{21} = \int_{x_a}^{x_b} \psi_i^{(2)} \tfrac{d\psi_j^{(1)}}{dx}\, dx, \\ K_{ij}^{22} = \int_{x_a}^{x_b} \left(\psi_i^{(2)} \psi_j^{(2)} + \tfrac{d\psi_i^{(2)}}{dx} \tfrac{d\psi_j^{(2)}}{dx} \right) dx, \quad K_{ij}^{23} = -\int_{x_a}^{x_b} \tfrac{1}{b} \tfrac{d\psi_i^{(2)}}{dx} \psi_j^{(3)}\, dx, \quad K_{ij}^{24} = 0, \\ K_{ij}^{31} = 0, \quad K_{ij}^{32} = -\int_{x_a}^{x_b} \tfrac{1}{b}\, \psi_i^{(3)} \tfrac{d\psi_j}{dx}\, dx, \quad K_{ij}^{33} = \int_{x_a}^{x_b} \left(\tfrac{1}{b^2} \psi_i^{(3)} \psi_j^{(3)} + \tfrac{d\psi_i^{(3)}}{dx} \tfrac{d\psi_j^{(3)}}{dx} \right) dx, \\ K_{ij}^{34} = -\int_{x_a}^{x_b} \tfrac{d\psi_i^{(3)}}{dx} \psi_j^{(4)}\, dx, \quad K_{ij}^{41} = -\int_{x_a}^{x_b} k\, \tfrac{d\psi_i^{(4)}}{dx} \psi_j^{(1)}\, dx, \quad K^{42} = 0, \\ K^{43} = -\int_{x_a}^{x_b} \psi_i^{(4)} \tfrac{d\psi_j^{(3)}}{dx}\, dx, \quad K_{ij}^{44} = \int_{x_a}^{x_b} \left(\psi_i^{(4)} \psi_j^{(4)} + \tfrac{d\psi_i^{(4)}}{dx} \tfrac{d\psi_j^{(4)}}{dx} \right) dx, \\ F_i^1 = \int_{x_a}^{x_b} kq\, \psi_i^{(1)}\, dx, \quad F_i^2 = 0, \quad F_i^3 = 0, \qquad F_i^4 = -\int_{x_a}^{x_b} q\, \tfrac{d\psi_i^{(4)}}{dx}\, dx \end{gathered} \tag{3.18}$$

4. Weak Form Galerkin Model: MWKFEMEB2

Here we consider the set of four equations in Eq. (3.12). The weak forms over a typical element are

$$\begin{aligned} 0 &= \int_{x_a}^{x_b} \left(k\delta w_h w_h + \tfrac{d\delta w_h}{dx} V_h - \delta w_h \, q \right) dx - \delta w_h(x_a) V_1 - \delta w_h(x_b) V_2 \\ 0 &= \int_{x_a}^{x_b} \left(\delta\theta_h V_h + \tfrac{d\delta\theta_h}{dx} M_h \right) dx - \delta\theta_h(x_a) M_1 - \delta\theta_h(x_b) M_2 \\ 0 &= \int_{x_a}^{x_b} \delta M_h \left(-\tfrac{M_h}{b} + \tfrac{d\theta_h}{dx} \right) dx \\ 0 &= \int_{x_a}^{x_b} \delta V_h \left(\theta_h + \tfrac{dw_h}{dx} \right) dx \end{aligned} \tag{3.19}$$

Since (w_h, θ_h, M_h, V_h) appear as the nodal variables, they all can be approximated by Lagrange interpolation functions. Let

$$\begin{aligned} w_h &= \textstyle\sum_{j=1}^{m} w_j \, \psi_j^{(1)}(x), \quad \theta_h = \sum_{j=1}^{n} \theta_j \, \psi_j^{(2)}(x), \\ M_h &= \textstyle\sum_{j=1}^{p} M_j \, \psi_j^{(3)}(x), \quad V_h = \sum_{j=1}^{q} V_j \, \psi_j^{(4)}(x), \end{aligned} \tag{3.20}$$

where w_j, θ_j, M_j, and V_j denote the nodal values of w_h, θ_h, M_h, and V_h, respectively, at the jth node. Substitution of Eq. (3.20) into Eq. (3.19), we obtain the finite element model

$$\begin{bmatrix} [K^{11}] & [K^{12}] & [K^{13}] & [K^{14}] \\ [K^{12}]^\top & [K^{22}] & [K^{23}] & [K^{24}] \\ [K^{13}]^\top & [K^{23}]^\top & [K^{33}] & [K^{34}] \\ [K^{14}]^\top & [K^{24}]^\top & [K^{34}]^\top & [K^{44}] \end{bmatrix} \begin{Bmatrix} \{u\} \\ \{\theta\} \\ \{M\} \\ \{V\} \end{Bmatrix} = \begin{Bmatrix} \{F^1\} \\ \{F^2\} \\ \{F^3\} \\ \{F^4\} \end{Bmatrix} \tag{3.21}$$

where

$$
\begin{gathered}
K_{ij}^{11}=\int_{x_a}^{x_b} k\psi_i^{(1)}\psi_j^{(1)}dx, \quad K_{ij}^{12}=0, \quad K_{ij}^{13}=0, \quad K_{ij}^{14}=\int_{x_a}^{x_b}\frac{d\psi_i^{(1)}}{dx}\psi_j^{(4)}\,dx, \\
K_{ij}^{21}=0, \quad K_{ij}^{22}=0, \quad K_{ij}^{23}=\int_{x_a}^{x_b}\frac{d\psi_i^{(2)}}{dx}\psi_j^{(3)}\,dx, \quad K_{ij}^{24}=\int_{x_a}^{x_b}\psi_i^{(2)}\psi_j^{(4)}\,dx, \\
K_{ij}^{31}=0, \quad K_{ij}^{32}=\int_{x_a}^{x_b}\psi_i^{(3)}\frac{d\psi_j^{(2)}}{dx}\,dx, \quad K_{ij}^{33}=-\int_{x_a}^{x_b}\frac{1}{b}\psi_i^{(3)}\psi_j^{(3)}\,dx, K^{34}=0 \\
K_{ij}^{41}=\int_{x_a}^{x_b}\psi_i^{(4)}\frac{d\psi_j^{(1)}}{dx}\,dx, \quad K^{42}=\int_{x_a}^{x_b}\psi_i^{(4)}\psi_j^{(2)}\,dx, \quad K^{43}=0, \quad K_{ij}^{44}=0, \\
F_i^1=\int_{x_a}^{x_b} q\,\psi_i^{(1)}\,dx+\psi_i^{(1)}(x_a)V_1+\psi_i^{(1)}(x_b)V_2, \\
F_i^2=\psi_i^{(2)}(x_a)M_1+\psi_i^{(2)}(x_b)M_2, \quad F_i^3=0, \quad F_i^4=0
\end{gathered}
\tag{3.22}
$$

B. Numerical Examples

1. Problem 1: Cantilever Beam

Consider a cantilever beam that is fixed on the left size (see Fig. 5). The modulus of elasticity and momen of inertia are 200x10^5 $\frac{kN}{m^3}$ and 29x10^6 mm^4. The right end has a 60kN downward force. There is also a downward linearly varying distributed load. The the left end the force is 24kn and on the right end it is 60kn.

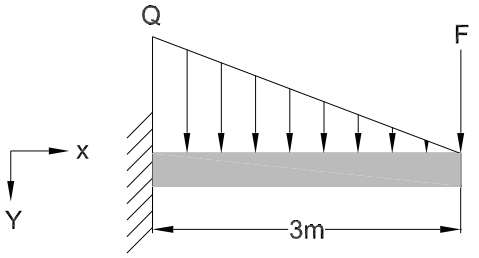

Fig. 5. Cantilever Beam with a Distributed and a Point Loads.

The problem has been solved using WGFEMEB and MSFEMEB1, both with two, four and eight hermite elements. The deflection and rotation results can be found in Tables IX and X.

Table IX. The Deflection (m) Results for Problem 1

		WGFEMEB			MLSFEMEB1		
x	Exact†	2H	4H	8H	2H	4H	8H
0.0000	0.0000	0.0000	0.0000	0.0000	0.0000	0.0000	0.0000
0.3750	0.0025			0.0025			0.0025
0.7500	0.0094		0.0094	0.0094		0.0094	0.0094
1.1250	0.0199			0.0199			0.0199
1.5000	0.0334	0.0334	0.0334	0.0334	0.0334	0.0334	0.0334
1.8750	0.0491			0.0491			0.0491
2.2500	0.0666		0.0666	0.0666		0.0666	0.0666
2.6250	0.0852			0.0852			0.0852
3.0000	0.1042	0.1043	0.1043	0.1043	0.1043	0.1043	0.1043

†Results taken from Reddy's *An Introduction to the Finite Element Method.* [1]

Table X. The Rotation (-θ) Results for Problem 1

x	Exact†	WGFEMEB			MLSFEMEB1		
		2H	4H	8H	2H	4H	8H
0.0000	0.0000	0.0000	0.0000	0.0000	0.0000	0.0000	0.0000
0.3750	0.0128			0.0128			0.0128
0.7500	0.0235		0.0235	0.0235		0.0235	0.0236
1.1250	0.0323			0.0323			0.0323
1.5000	0.0393	0.0393	0.0393	0.0393	0.0393	0.0393	0.0393
1.8750	0.0446			0.0446			0.0446
2.2500	0.0483		0.0483	0.0483		0.0483	0.0483
2.6250	0.0505			0.0505			0.0505
3.0000	0.0512	0.0512	0.0512	0.0512	0.0512	0.0512	0.0512

†Results taken from Reddy's *An Introduction to the Finite Element Method.* [1]

The bending moment diagram is given in Figure 6. The exact solution was taken from Reddy's book:*An Introduction to the Finite Element Method.* [1] Figure 7 shows the shear diagram.

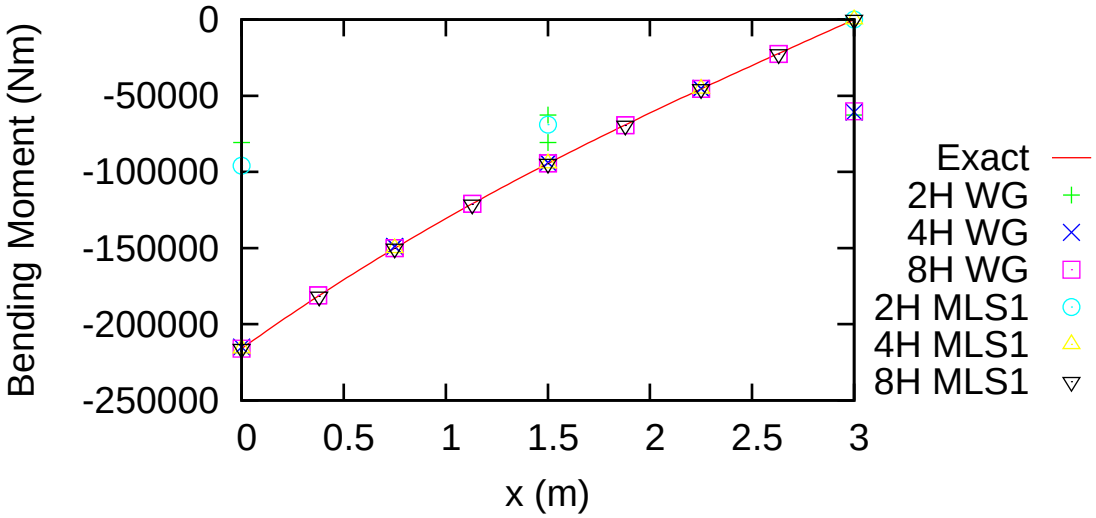

Fig. 6. Bending Moment Diagram for Problem 1.

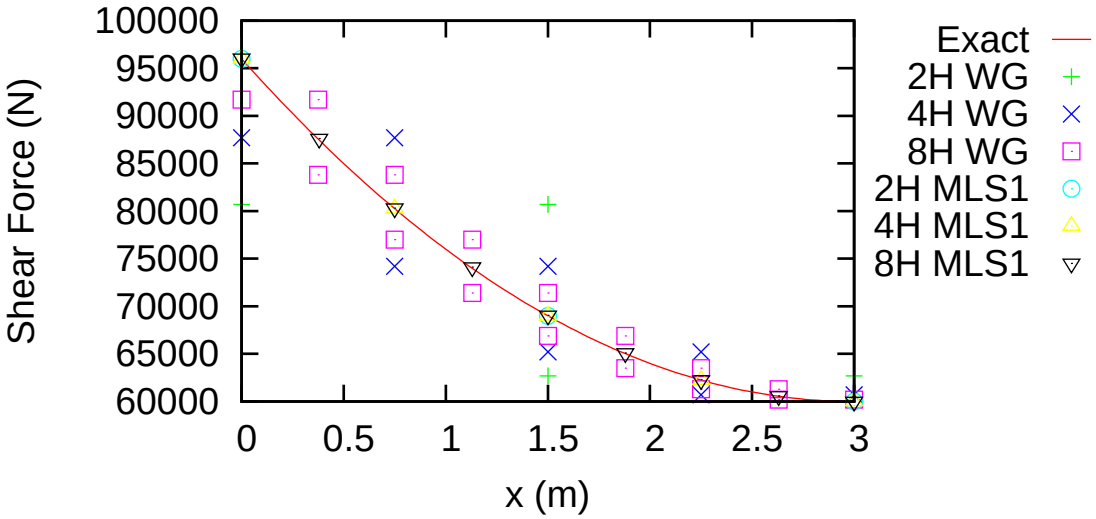

Fig. 7. Shear Diagram for Problem 1.

2. Problem 2: Simply Supported Beam

Consider a simply supported beam that is 6m long (see Fig. 8). The modulus of elasticity is 200x10^5 $\frac{kN}{m^3}$ and the moment of inertia is 29x10^6 mm^4. The beam is pinned on the left and and is supported on the right end. There is a 60kN downward force in the middle of the beam.

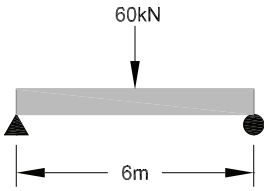

Fig. 8. Simply Supported Beam with a Point Load.

The problem has been solved using WGFEMEB and MSFEMEB1, both with two, four and eight hermite elements. The deflection and rotation results can be found in Tables XI and XII. The bending moment and shear force diagrams are Figure 9 and Figure 10 respectively.

Table XI. The Deflection (m) Results for Problem 2

x	Exact†	WGFEMEB			MLSFEMEB1		
		2H	4H	8H	2H	4H	8H
0.0000	0.0000	0.0000	0.0000	0.0000	0.0000	0.000	0.0000
0.7500	0.0171			0.0171			0.0171
1.5000	0.0320		0.0320	0.0320		0.0320	0.0320
2.2500	0.0426			0.0426			0.0426
3.0000	0.0466	0.0466	0.0466	0.0466	0.0466	0.0466	0.0466
3.7500	0.0426			0.0426			0.0426
4.5000	0.0320		0.0320	0.0320		0.0320	0.0320
5.2500	0.0171			0.0171			0.0171
6.000	0.0000	0.0000	0.0000	0.0000	0.0000	0.0000	0.0000

† The exact solution was taken from *Mechanics of Materials.* [3]

Table XII. The Rotation (-θ) Results for Problem 2

x	Exact	WGFEMEB			MLSFEMEB1		
		2H	4H	8H	2H	4H	8H
0.0000	0.0232	0.0258	0.0233	0.0233	0.0233	0.0233	0.0233
0.7500	0.0218			0.0218			0.0218
1.5000	0.0175		0.0175	0.0175		0.0175	0.0175
2.2500	0.0102			0.0102			0.0102
3.0000	0.0000	-0.0217	0.0000	0.0000	0.0000	0.0000	0.0000
3.7500	-0.0102			-0.0102			-0.0102
4.5000	-0.0175		-0.0175	-0.0176		-0.0175	-0.0175
5.2500	-0.0218			-0.0218			-0.0218
6.000	-0.0232	-0.0208	-0.0233	-0.0233	-0.0233	-0.0233	-0.0233

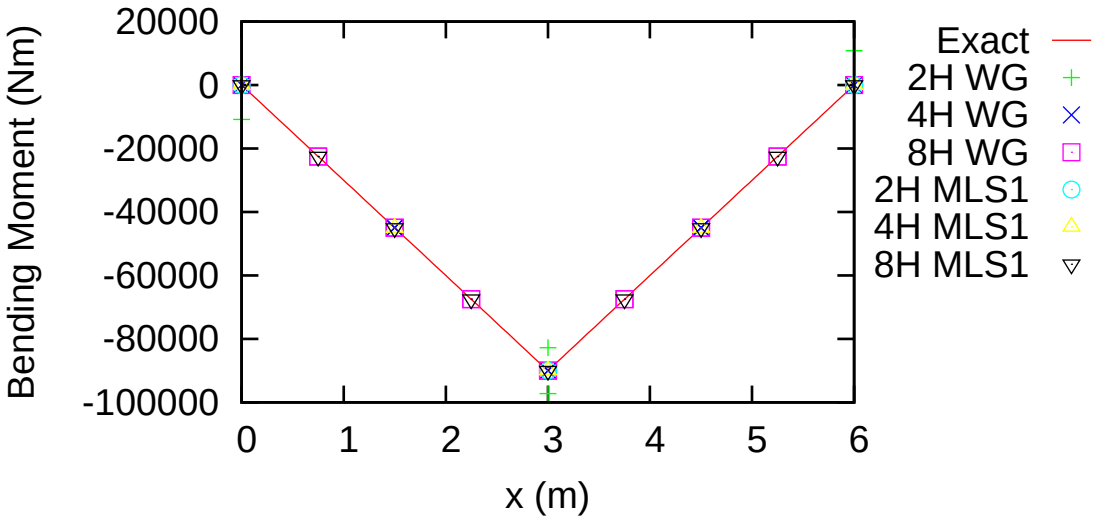

Fig. 9. Bending Moment Diagram for Problem 2.

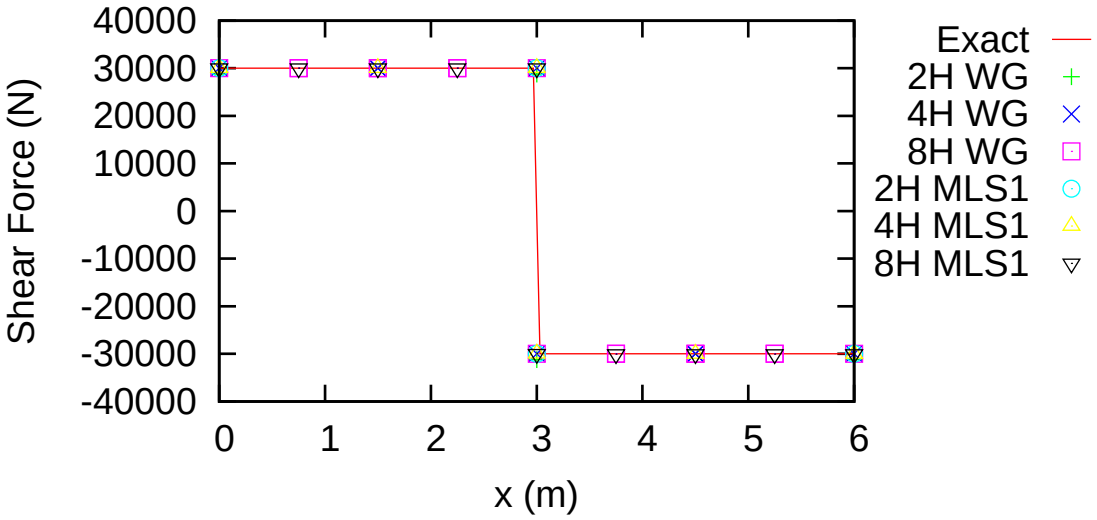

Fig. 10. Shear Diagram for Problem 2.

3. Problem 3: Fixed Beam

Consider a 2m long beam that is fixed on both ends (see Fig. 11). The modulus of elasticity and the moment of inertia are 25 $\frac{kN}{m^3}$ and 1 mm^4 respectively. There is a cubicly varying downward distributed load that is symmetric about the center of the beam. The problem has been solved using WGFEMEB and MSFEMEB1, both with

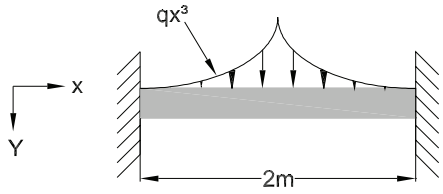

Fig. 11. Fixed Beam with a Distributed Load.

two, four and eight hermite elements. The deflection, rotation, bending moment and shear force results can be found in Tables XIII, XIV, XV and XVI. The bending moment and shear force diagrams are Figure 12 and Figure 13 respectively.

Table XIII. The Deflection (m) Results for Problem 3 Solved Using the Half Beam Model

x	Exact	MLSFEMEB1		
		2H	4H	8H
0.00000	0.00000	0.00000	0.00000	0.00000
0.12500	0.00033			0.00033
0.25000	0.00120		0.00120	0.00120
0.37500	0.00240			0.00240
0.50000	0.00375	0.00376	0.00375	0.00375
0.62500	0.00506			0.00506
0.75000	0.00616		0.00616	0.00616
0.87500	0.00689			0.00689
1.00000	0.00714	0.00716	0.00714	0.00714

Table XIV. The Rotation (-θ) Results for Problem 3 Solved Using the Half Beam Model

x	Exact	MLSFEMEB1		
		2H	4H	8H
0.00000	0.00000	0.0000	0.00000	0.00000
0.12500	0.00505			0.00505
0.25000	0.00854		0.00854	0.00854
0.37500	0.01048			0.01048
0.50000	0.01089	0.01091	0.01089	0.01089
0.62500	0.00983			0.00983
0.75000	0.00747		0.00747	0.00747
0.87500	0.00405			0.00405
1.00000	0.00000	0.0000	0.00000	0.00714

Table XV. The Moment (kn m) Results for Problem 3 Solved Using the Half Beam Model

x	Exact	MLSFEMEB1		
		2H	4H	8H
0.00000	-0.11667	-0.11693	-0.11668	-0.11667
0.12500	-0.08541			-0.08541
0.25000	-0.05422		-0.05423	-0.05422
0.37500	-0.02329			-0.02329
0.50000	0.00677	0.00651	0.00676	0.00677
0.62500	0.03481			0.03481
0.75000	0.05897		0.05895	0.05897
0.87500	0.07644			0.07644
1.00000	0.08333	0.08307	0.08332	0.08333

Table XVI. The Shear Force (-kN) Results for Problem 3 Solved Using the Half Beam Model

x	Exact	MLSFEMEB1		
		2H	4H	8H
0.00000	-0.25000	-0.25000	-0.25000	-0.25000
0.12500	-0.24994			-0.24994
0.25000	-0.24902		-0.24902	-0.24902
0.37500	-0.24506			-0.24506
0.50000	-0.23438	-0.23437	-0.23437	-0.23437
0.62500	-0.21185			-0.21185
0.75000	-0.17090		-0.17090	-0.17090
0.87500	-0.10345			-0.10345
1.00000	0.00000	0.00000	0.00000	0.00000

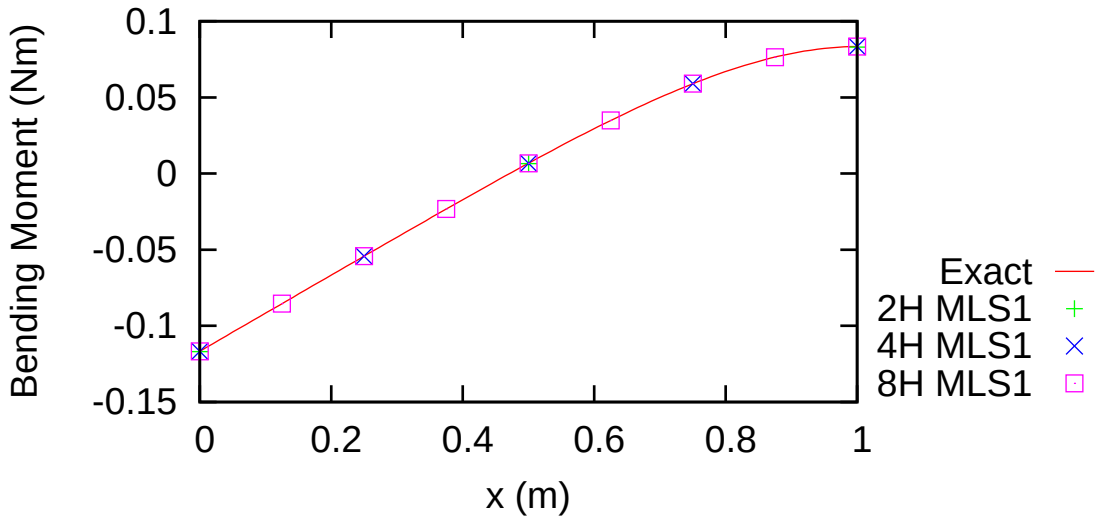

Fig. 12. Bending Moment Diagram for Problem 3.

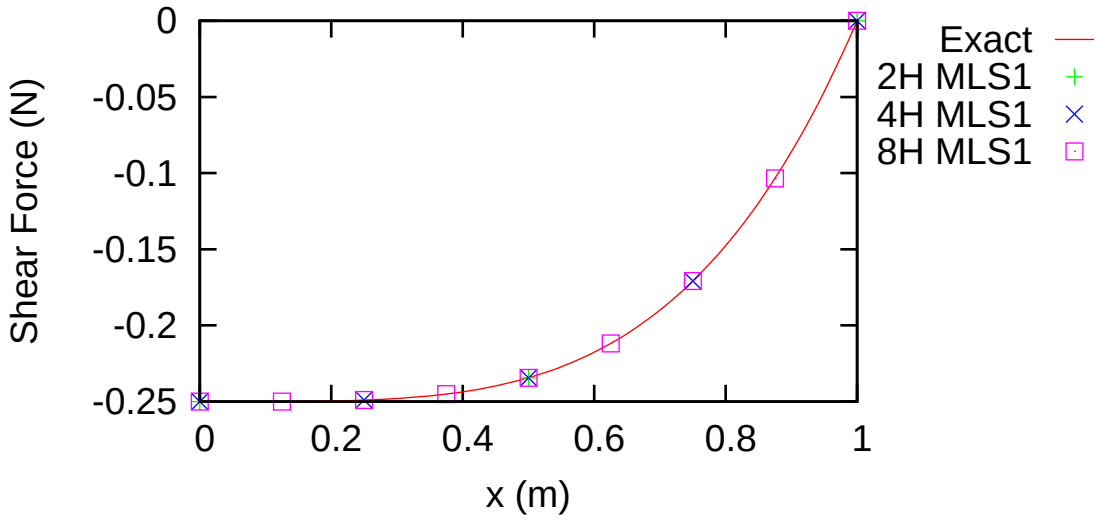

Fig. 13. Shear Diagram for Problem 3.

C. Conclusions

The value of the primary variables calculated using WGFEMEB and MLSFEMEB1 were almost an exact match to the exact solution in example one and two. In example three, the MLSFEMEB1 model calculated the exact solution. The secondary

variables were not accurately calculated with the WGFEMEB while the MLSFE-MEB1 model calculated accurate values. Future work will include implimention of the MLSFEMEB2, MWGFEMEB1, MWGFEMEB2 model and producing numerical results.

CHAPTER IV

CONCLUSIONS AND FUTURE WORK

A. Summary and Concluding Remarks

In this work the least squares finite element models were developed and applied to the one-dimensional heat transfer and Euler Bernoulli beam theory (EBT) problems. Two models were developed for the one-dimensional heat transfer problem. the first (LSFEMHT) used the full form of the governing equation while the second (MLSFEMHT) used the mixed form. Weak form Galerkin models were included for the same forms of the governing equation (WGFEMHT, MWGFEMHT). Two finite element models were also developed for the Euler-Bernoulli beam theory. Both models used a mixed form of the governing equation, the first was the second order form (MLSFEMEB1), and the other was the first order form. Again, weak form Galerkin models were included for the same forms of the governing equations. Numerical examples were presented for both problems.

Four examples for the one-dimensional heat transfer problem were presented, they include: a simple differential equation, heat transfer in a fin, heat transfer in a rod and axisymmetric heat in a cylinder. When primary variables are computed using WGFEMHT and LSFEMHT the results are comparable when there are the same number of degrees of freedom. To get similar results with the MLSFEMHT model, quadratic or higher order shape functions are required. When computing the secondary variable with LSFEMHT or LSFEMHT with second order shape functions, the results are more accurate than the WGFEMHT. Also, the results from the WGFEMHT are not continuous unlike the least squares models.

Numerical examples for the EBT include: a cantilever beam, a simply supported

beam and a beam that was fixed on both ends. The first two examples were solved with the MLSFEMEB1 model and a weak form Galerkin model using the full form of the governing equation (WGFEMEB), while the third problem was only solved using the MLSFEMEB1 model. Both the MLSFEMEB1 and WGFEMEB models computed accurate results when solving the primary variables. The MLSFEMEB1 model computed accurate results for the secondary variables while the WGFEMEB model results were not as accurate.

In conclusion, the least squares models are a viable option when solving one-dimensional heat transfer and EBT problems numerically. Least squares models accurately calculate the primary and secondary variables as compared to the weak form Galerkin models which only compute primary variables with the same accuracy. In the field of design, the secondary variables are as important if not more important than the primary variables. It is a major advantage the least squares model has over the weak form Galerkin mode.

B. Future Work

The least squares model has already been used in fluid flow, though very little work has been done with it in solid mechanics. In this work several models were presented for one-dimensional equations of heat transfer and beam bending. The present study may be extened to Timoshenko beam theory and multidimensional problems as well as nonlinear problems.[4] Another area of future work is to couple the least squares model with meshless shape functions. Lui, Zhang and Lu have done this with heat transfer probems ([5],[6]), while others have done this with fluid flow. As with the finite element shape functions, there is very little work that has been done in the area of solid mechanics.

REFERENCES

1. Reddy JN. *An Introduction to the Finite Element Method*. 3rd edn., McGraw-Hill Series in Mehanical Engineering, McGraw-Hill: Boston, 2006.

2. Reddy JN. *Energy Principles and Variational Methods in Applied Mechanics*. 2nd edn., McGraw-Hill: Boston, 2002.

3. Beer FP, E Russell Johnston J, DeWolf JT. *Mechanics of Materials*. 3rd edn., McGraw-Hill: Boston, 2002.

4. Reddy JN. *An Introduction to Nonlinear Finite Element Analysis*. Oxford University Press: Oxford England, 2004.

5. Liu Y, Zhang X, Lu M. Meshless least-squares method for solving the steady-state heat conduction equation. *Tsinghua Science and Technology* Feb 2005; **10**(1):61–68.

6. Lui Y, Zhang X, Lu MW. A meshless method based on least-squares approach for steady- and unsteady-state heat conduction problems. *Numerical Heat Transfer, Part B* 2005; **47**:257–275.

VITA

Brittan Sheldon Pratt

Address: Texas A&M University
Department of Mechanical Engineering
c/o Dr. J. N. Reddy
3213 TAMU
College Station, TX 77843-3213

Education: M.S., Mechanical Engineering, Texas A&M University, 2008
B.M.E., Mechanical Engineering, Grove City College, 2003